We are IntechOpen, the world's leading publisher of Open Access books Built by scientists, for scientists

4,800
Open access books available

122,000
International authors and editors

135M
Downloads

Our authors are among the

154
Countries delivered to

TOP 1%
most cited scientists

12.2%
Contributors from top 500 universities

CLARIVATE ANALYTICS BOOK CITATION INDEX INDEXED

WEB OF SCIENCE™

Selection of our books indexed in the Book Citation Index in Web of Science™ Core Collection (BKCI)

Interested in publishing with us?
Contact book.department@intechopen.com

Numbers displayed above are based on latest data collected.
For more information visit www.intechopen.com

6

σ-Bonded *p*-Dioxolene Transition Metal Complexes

Anastasios D. Keramidas[1], Chryssoula Drouza[2] and Marios Stylianou[1]
[1]*University of Cyprus*
[2]*Cyprus University of Technology*
Cyprus

1. Introduction

Hydroquinones(HQ) are molecules of great importance in chemistry and biology. They undergo proton-coupled electron transfer to afford neutral *p*-semiquinone(SQ) and *p*-quinone(Q) species as illustrated in figure 1.

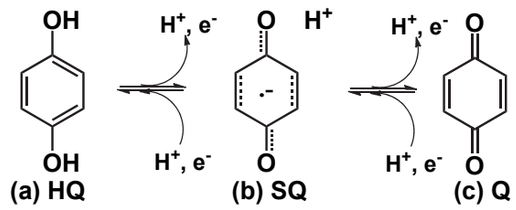

Fig. 1. Proton-coupled electron transfer in hydroquinone molecules

Metal ions are known to lie in close proximity with these species in biological systems, thus resulting in immediate interaction. The two coupled, metal and organic redox centers have been found to participate in several biological processes such as, the oxidative maintenance of biological amine levels, (Klinman, 1996) tissue (collagen and elastin) formation, (Klinman, 1996) photosynthesis (Calvo, et al., 2000) and respiration (Iwata, et al., 1998). Although the crystal structures of many of these enzymes have been solved, the role of the metal ions in these reactions is still controversial. From another point of view, quinonoid metal complexes exhibit rich redox, magnetic and photochemical properties and thus can underpin key technological advances in the areas of energy storage, sensors, catalysis and "smart materials" (Evangelio & Ruiz-Molina, 2005; Stylianou, et al., 2008).

Metal ions interact with hydroquinone systems, through σ-bonding to the oxygen atoms and/or through π-bonding to the carbocyclic ring. The structurally characterized σ-bonded hydroquinone metal complexes are surprisingly limited. Structures of metal ions with *p*-semiquinones and quinones are even rarer, mainly due to the absence of a chelate coordination site in simple *p*-(hydro/semi)quinone and the low p*K* values of the semiquinone and quinone oxygen atoms. A strategy to synthesize stable metal complexes with hydroquinone species is to use substituted hydroquinones in *o*-position with substituents containing one or more donor atoms, enabling in this way the metal atom to

form chelate rings. In addition to the stabilization of the metal complexes, hydroquinones substitution offers a direct control of the redox properties of the metal ion and increases the number of new possible structural motives by changing the number and the type of the donor atoms of the chelating group. One of the problems that someone has to face working with "non-innocent" ligands, such as hydroquinones, is the determination of their formal charge in the complex. Sometimes, physicochemical properties of the complexes, such as strong magnetic coupling between the metal ion and the organic radical, may give misleading results regarding the oxidation states. It has been shown that X-ray crystallography can be used for the determination of the oxidation states of the non innocent ligands in the complexes. For example, the $C\text{-}O_{hydroquinonate}$ and the C-C bond lengths of the *p*-dioxolene ligands are strongly dependent on the formal charge of the ligands.

In this chapter we demonstrate that the rich structural chemistry of hydroquinonate complexes is predicated on a) the ability of the metal ions to reversibly deprotonate the –OH groups, b) the remote and adjacent bridge ligating modes of hydroquinone and c) the reversible metal ion – hydroquinone electron transfer which results in stabilization of the *p*-semiquinone oxidation state. The determination of the oxidation state of the *p*-dioxolene ligand based of C-O and intraring bond distances is also analyzed. The application of a statistical approach for the determination of the ligand formal charges is being discussed. In addition, a graphical method for the assignment of the oxidation states has been included in this chapter. Finally, the factors that promote the stabilization of the semiquinone radical versus the hydroquinone are discussed based on the structural data. Here, we will mainly focus on the $V^{IV/V}$ complexes with the 2,5- bisubstituted hydroquinone with iminodiacetic acid or bis(2-methylpyridyl)amine in *o*-position. These are the only universally structurally characterized *p*-semiquinone examples in the literature up to today and the structure of the hydroquinone complexes can be directly compared with that of the *p*-semiquinone analogues. These compounds are oxidized from the atmospheric oxygen to form stable semiquinone radicals, trapping intermediates of dioxygen reduction that have been identified by X-ray crystallography. This is an important development towards the better understanding of the catalytic reduction mechanisms of dioxygen from metal ions in biological systems as well as in the catalytic oxidation of organic substrates from metal complexes.

It is clear that σ-bonded hydroquinone/*p*-semiquinone-metal complexes have many interesting properties that have only begun to be explored or exploited (*vide infra*). X-ray crystallography represents a basic and irreplaceable tool in this exploration. This chapter will provide a glimpse of the fascinating structural chemistry exhibited by hydroquinones/*p*-semiquinones metal complexes and the utilization of X-ray crystallography into the exploration of the chemistry and the development of hydroquinones/*p*-semiquinones based functional bioinorganic models.

2. Structural studies of hydroquinonate/p-semiquinonate/p-quinone transition metal complexes

Structural investigation has proven to be an essential tool for the characterization of *p*-dioxolene complexes. Metal-oxygen bond lengths are often characteristic of a particular oxidation state of the metal, and the *p*-dioxolene carbon-oxygen lengths are sensitive to the charge of the ligand. Apart from providing indirect information on the charge distribution within the complex, crystallographic studies have revealed the donor-acceptor tendency for

complexation. The first hydroquinone complex characterized by crystallography has been reported 30 years ago (Heistand, et al., 1982). However only the last 10 years the number of the characterized by crystallography *p*-dioxolene complexes has increased significantly, including the first *p*-semiquinone complex in 2002 (Drouza, et al., 2002). This is in marked contrast to the extensive structural chemistry of chelate stabilized *o*-dioxolene metal complexes reported in the literature(Pierpont, 2001). This is mainly due to the absence of a chelate coordination site in simple *p*-dioxolenes and their low pKa values. The oxygen atoms of *p*-dioxolenes act as unidentate donor atoms, as shown in figure 2 for hydroquinones. Hydroquinone may ligate one metal ion or two metal ions bridged from two different or from the same oxygen donor atoms (figure 2).

Substituted in *o*-position *p*-dioxolenes, with substituents containing one or more donor atoms, stabilize metal ion ligation through the formation of chelate rings. A systematic collection of the substituents reported in the literature including their transition metal complexes characterized by X-ray crystallography is illustrated in figure 3. The transition metal complexes of these ligands together with some important crystallographic data are summarized in table 1. The type of the substituent is very important because it may control the stabilization of certain metal ions defining the oxidation states of the metal ions and of the *p*-dioxolenes, as well the structure of the molecule.

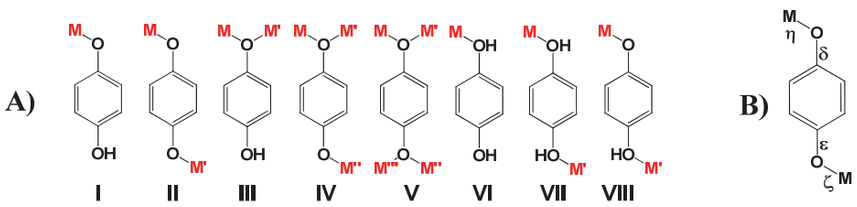

Fig. 2**.** A) Coordination modes of hydroquinones **I**) monodentate, **II**) remote bridged, **III**) adjacent bridged, **IV**) remote and one adjacent bridges, **V**) remote and two adjacent bridges **VI**) protonated monodentate, **VII**) protonated bridged, **VIII**) monoprotonated bridged, B) Labeling of the M-O and C-O bonds

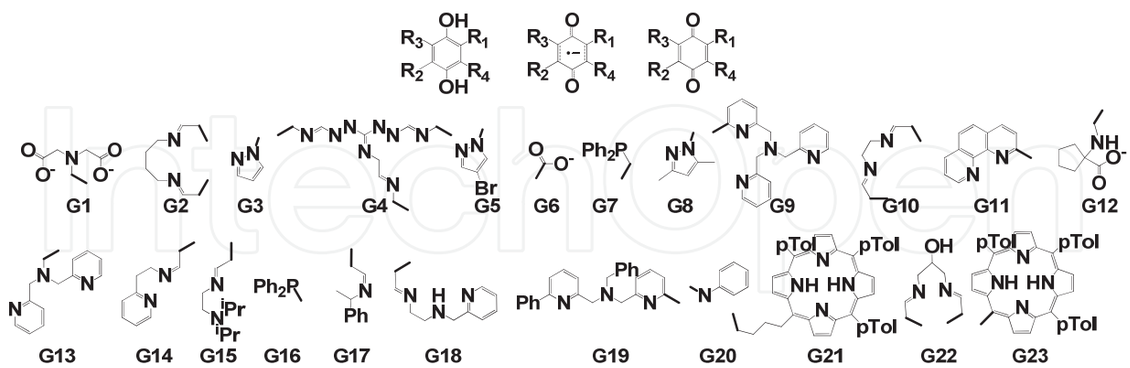

Fig. 3. Substituents of hydroquinone / *p*-semiquinone / *p*-quinones used for transition metal ion ligation

Comp	Metal	η / Å	δ / Å	ε / Å	ζ / Å	C-O-M (°)	Arom. Substitution	Ref.
1[a]	Fe^{III}	1.903(4) 1.864(4)	1.374(8) 1.372(8)	1.316(6) 1.330(7)	---	126.7(3) 129.6(3)	R1=G2 R2=R3=R4=H	(Sanmartin, et al., 2004)
2[a]	Ti^{III}	1.828(8) 1.775(8)	1.38(3) 1.38(2)	1.34 (1) 1.35(2)	---	146.5(7) 138.5(8)	R1=R2=R3=R4=H	(Errington, et al., 2007)

3[a]	Pt^{II}	2.030(3)	1.380(6)	1.334(5)	---	130.3 (3)	R1=G7 R2=R3=R4=H	(Sembiring, et al., 1999)
4[a]	Cu^{II}	1.900(4)	1.386(7)	1.327(7)	---	122.0(3)	R1=G9 R2=R3=R4=H	(He, et al., 2003)
5[a]	Cu^{II},I	1.924(1)	1.381(3)	1.329(2)	---	126.4(1) 127.2(1)	R1=G10 R2=R3=R4=H	(Margraf, et al., 2006)
6[a]	Ni^{II}	1.854(2) 1.860(3)	1.397(5) 1.386(5)	1.321(5) 1.322(4)	---	127.8 (2) 127.6(2)	R1=G10 R3= tBu R2=R4=H	(Margraf, et al., 2006)
7[a]	Pd^{II}	1.940(7)	1.39(1)	1.34(1)	---	124.5(5)	R1=G11 R2=R3=R4=H	(Berthon, et al., 1992)
8[a]	Cr^{III}	1.924(2)	1.391(3)	1.362(3)	---	120.9(1)	R1=G1 R2=R3=R4=H	(Huang, et al., 2008)
9[a]	Fe^{III}	1.927(2), 1.920(2)	1.379(4)	1.343(4)	---	127.7(2), 126.4(2)	R1= G17, R2=R3=R4=H	(Becker, et al., 2010)
10[a]	Ni^{II}	1.827(4) 1.827(4)	1.386(9) 1.393(8)	1.332(7) 1.325(7)	---	127.3(3), 127.4(3)	R1= G10, R2=R3=R4=H	(Kondo, et al., 2003)
11[a]	Cu^{II}	1.870(4)	1.384(9)	1.321(7)	---	126.0(4)	R1= G18, R2=R3=R4=H	(Li, et al., 2000)
12[a]	Ni^{II}	1.90(1) 1.87(1)	1.38(2) 1.36(2)	1.37(2) 1.35(5)	---	119.8(8), 118.9(8)	R1= G7, R2=R3=R4=H	(Sembiring, et al., 1992)
13[a]	Mo^{VI}	1.945(2) 1.955(2)	1.381(6) 1.359(5)	1.353(5) 1.348(5)	---	137.8(2), 133.5(2)	R1= G6, R2=R3=R4=H	(Litos, et al., 2006)
14[a]	W^{VI}	1.88(3)	1.36(4)	1.36(4)	---	166(2), 157(3),	R1=R2=R3=R4=H	(Vaid, et al., 2001)
15[b]	V^{IV}	1.887(4) 1.887(4)	1.322(6)	1.322(6)	---	137.0(1), 137.0(1)	R1=R2=G1 R3=R4=H	(Drouza, et al., 2002)
16[b]	V^{V}	1.878(3) 1.865(3)	1.353(6) 1.353(5)	1.352(6) 1.353(5)	1.878(3) 1.865(3)	131.9(3) 131.5(3)	R1=R2=G1 R3=R4=H	(Drouza, et al., 2002)
17[b]	W^{V}	1.948(6)	1.362(9)	1.362(9)	1.948(6)	133.3(5), 133.3(5)	R1=R2=R3=R4=H	(Stobie, et al., 2003)
18[b]	Cu^{II}	1.803(3)	1.300(2)	1.300(2)	1.803(3)	126.8(1), 126.8(1)	R1=R2=G3 R3=R4=H	(Dinnebier, et al., 2002)
19[b]	Fe^{III}	1.862(1)	1.3492(4)	1.3492(4)	1.8616(1)	132.13(3), 132.13(3)	R1=R2=R3=R4=H	(Heistand, et al., 1982)
20[b]	Cu^{I}	1.91(2) 1.916(2)	1.322(3) 1.327(3)	1.322(3) 1.327(3)	1.91(2) 1.916(2)	123.9(2) 122.6(2)	R1=R2=G5 R3=R4=H	(Margraf, et al., 2009)
21[b]	Ru^{III}	1.975(7)	1.38(1)	1.34 (1)	1.966(5)	115.9 (6)	R1=R2=G8 R3=R4=H	(Kumbhakar, et al., 2008)
22[b]	Ru^{III}	1.983(2)	1.346(4)	1.346(4)	1.976(2)	118.4(2), 115.9(2)	R1=R2=G8 R3=R4=H	(Kumbhakar, et al., 2008)
23[b]	Cu^{II}	1.915(1)	1.322(2)	1.322(2)	1.915(1)	121.4(1), 121.4(1)	R1=R2=G3 R3=R4=H	(Margraf, et al., 2006)
24[b]	Ti^{II}	1.785(5)	1.360(8)	1.360(8)	1.785(5)	165.1 (4) 165.1 (4)	R1=R4=Me R2=R3=H	(Arévalo, et al., 2003)
25[b]	Mn^{III}	2.193(4)	1.253(7)	1.253(7)	2.193(4)	180.000	R1=R2= R3=R4=Cl	(Brandon, et al., 1998)
26[b]	V^{IV}	1.951(3) 1.952(3)	1.364(5) 1.352(5)	1.364(5) 1.352(5)	1.951(3) 1.952(3)	128.2(3), 128.2(3)	R1=R2=G1 R3=R4=H	(Drouza & Keramidas, 2008)
27[b]	V^{V}	1.866(2) 1.824(2)	1.346(3) 1.346(3)	1.338(3) 1.338(3)	1.824(2) 1.866(2)	132.3(1), 137.0(1)	R1=R2=G1 R3=R4=H	(Drouza & Keramidas,

						137.0(1), 132.3(1)		2008)
28[b]	V^{V}	1.827(2) 1.823(2)	1.346(3) 1.325(3)	1.335(3) 1.327(3)	1.865(2) 1.878(2)	137.8(2), 132.3(2) 137.2(2), 135.9(2)	R1=R2=G1 R3=R4=H	(Drouza & Keramidas, 2008)
29[b]	$V^{IV/V}$	1.937(2) 1.879(2)	1.314(3) 1.350(4)	1.308(3) 1.345(4)	1.880(2) 1.879(2)	138.1(2), 136.4(2) 134.8(2), 131.8(2)	R1=R2=G1 R3=R4=H	(Drouza & Keramidas, 2008)
30[b]	$V^{IV/V}$	1.884(2) 1.898(3)	1.338(4) 1.302(4)	1.350(4) 1.303(4)	1.8512(2) 1.913(2)	134.3(2), 134.8(2)	R1=R2=G1 R3=R4=H	(Drouza & Keramidas, 2008)
31[b]	V^{III}	1.877(9)	1.38(2)	1.34(2)	1.886(7)	134.1(9), 129.9(8)	R1=R2=R3=R4=H	(Tanski & Wolczanski, 2001)
32[b]	Ti^{IV}	1.882(4) 1.915(6)	1.373(8) 1.37(1)	1.373(8) 1.36(1)	1.882(4) 1.874(6)	137.4(4), 137.4(4)	R1=R2=R3=R4=H	(Vaid, et al., 1997)
33[b]	Zr^{IV}	1.978(2)	1.357(3)	1.357(3)	1.978(2)	144.8(1), 144.8(1)	R1=R2=R3=R4=H	(Evans, et al., 1998)
34[b]	Ti^{III}	1.870(3),	1.360(7)	1.369(7)	1.898(4)	148.5(3), 1.429(3)	R1=R2=R3=R4=H	(Tanski, et al., 2000)
35[b]	Mo^{IV}	1.924(8) 1.974(8) 1.924(8)	1.34(2) 1.37 (2) 1.33 (2)	1.33(2) 1.38 (2) 1.34(2)	1.937(8) 1.935(8) 1.92(1)	137.3(9), 142.3(9) 127.5(9),	R1=R2=R3=R4=H	(McQuillan, et al., 1998)
36[b]	Cu^{II}	1.880(3)	1.337(5)	1.337(5)	1.88(3)	127.2(2), 127.2(2)	R1=G15 R2=R3=R4=H	(Kretz, et al., 2006)
37[b]	Ti^{III}	1.865(2), 1.867(2)	1.349(4)	1.348(4)	1.867(2)	165.3(2), 169.6(2)	R1=R2=R3=R4=H	(Horacek, et al., 2010)
38[b]	Ti^{III}	1.864(4), 1.86(4)	1.353(3)	1.353(3)	1.864(4)	155.2(2), 155.2(2)	R1=R2=R3=R4=H	(Kunzel, et al., 1996)
39[b]	Cu^{II}	2.370(3), 2.464(2)	1.386(4)	1.380(4)	2.370(3), 2.464(2)	111.7(2), 112.1(2)	R1=R2= G1, R3=R4=H	(Stylianou, et al., 2008)
40[b]	Pd^{II}	1.981(2)	1.341(4)	1.341(4)	1.981(2)	118.3(2)	R1=R2= G7, R3=R4=H	(Caldwell, et al., 2008)
41[b]	Mo^{VI}	1.922(8)	1.35(1)	1.35(1)	1.922(8)	136.1(7)	R1=R2=R3=R4=H	(Ung, et al., 1996)
42[b]	W^{VI}	1.93(1)	1.36(2)	1.36(2)	1.927(1)	137(1)	R1=R2=R3=R4=H	(McQuillan, et al., 1996)
43[b]	Cu^{II}	1.880(3)	1.337(5)	1.337(5)	1.880(3)	127.2(2)	R1=R2= G15, R3=R4=H	(Kretz, et al., 2006)
45[b]	Fe^{III}	1.874(8)	1.27(1)	1.27(1)	1.874(8)	169.4(7)	R1=R2=R3=R4=Cl	(Rheingold & Miller, 2003)
46[b]	Mo^{V}	1.948(9) 1.954(8)	1.36 (2) 1.36 (2)	1.38(2) 1.35(2)	1.914(8) 1.953(8)	140.9(8), 135.6(8)	R1=R2=R3=R4=H	(Ung, et al., 1999)
47[c]	Cu^{II}	1.889(7), 2.326(7)	1.40(2) 1.36(2)	1.32(1) 1.31(1)	---	121.1(5), 127.6(5),	R1= G4 R2=R3=R4=H	(Zharkouskaya, et al., 2005)
48[c]	Zn^{II}	2..021(3), 2.030 (3)	1.347(5)	1.347(5)	2..021(3), 2.030 (3)	123.2(2), 1233(2)	R1=R2=G6 R3=R4=H	(Rosi, et al., 2005)
49[c]	Cu^{II}	1.924(2), 1.980(2)	1.527(6)	1.347(4)	---	132.8(2), 121.7(2)	R1=G22 R2=R3=R4=H	(Song, et al., 2007)
50[c]	Cu^{II}	1.934(2), 1.930(3)	1.364(3)	1.371(4)	---	134.4(2), 1203(2)	R1=G12 R2-R3=R4=H	(Sreenivasulu, et al., 2006)
51[c]	Ti^{IV}	2.048(3),	1.373(7)	1.371(6)	---	126.2(3),	R1=G12	(Vaid, et al.,

		2.043(3)				126.8(3)	R2-R3=R4=H	1997)
g		1.782(3)	1.387(6)	1.361(6)	2.208(4)	173.0(3), 125.9(3)	R1=R2=R3=R4=H	(Vaid, et al., 1997)
b		1.794(4)	1.376(6)	1.351(6)	1.923(3)	164.1(3), 129.3(3)	R1=R2=R3=R4=H	(Vaid, et al., 1997)
52c	Cu^{II}	1.971(6), 1.955(7) 1.922(7), 1.929(7)	1.38(1)	1.32(2)	---	130.1(5), 130.1(6)	R1=G14 R2=R3=R4=H	(Gelling, et al., 1990)
53a	Zn^{II}	1.946(5) 1.962(6)	1.37(1) 1.39(1)	1.33(1) 1.35(1)	---	126.8(5) 123.8(5)	R1=G2 R2=R3=R4=H	(Matalobos, et al., 2004)
c		2.046(5) 2.043(5)	1.377(9) 1.368(8)	1.343(9) 1.327(8)	---	126.1(5), 127.4(5) 124.0(5), 128.8(5)	R1=G2 R2=R3=R4=H	(Matalobos, et al., 2004)
54c	Cu^{II}	1.893(2), 2.463(2)	1.374(4)	1.345(3)	---	118.0(2), 126.8(2)	R1= G19, R2= R3=R4=H	(Matalobos, et al., 2004)
55c	Cu^{II}	1.936(6), 1.978(6), 2.358(6), 1.945(6)	1.39(1), 1.37(1)	1.36(1), 1.35(1)	---	129.9(6), 119.2(5), 108(5), 128.8(5)	R1= G1, R2= R3=R4=H	(Stylianou, et al., 2008)
56c	Cu^{II}	1.971(6), 1.934(6)	1.389(9)	1.350(8)	---	128.1(5), 132.1(6)	R1= G18, R2=R3=R4=H	(Li, et al., 2000)
57c	Pd^{II}	2.02(2), 2.13(1)	1.40(4)	1.36(3)	---	118(1), 122(1)	R1= G7, R2=R3=R4=H	(Sembiring, et al., 1995)
58c	Cu^{II}	1.971(6), 1.955(7)	1.38(1)	1.32(1)	---	130.1(5), 130.1(6)	R1=R3= G14, R2=R4=H	(Gelling, et al., 1990)
59d	Ti^{IV}	2.07(1), 2.014(7)	1.38(2)	1.37(2)	1.78(1)	126.6(7), 126(1), 153(1)	R1=R2=R3=R4=H	(Vaid, et al., 1999)
d		2.014(7), 2.07(1)	1.382)	1.37(2)	1.78(1)	126.6(7), 126(1), 153(1)		
b		1.836(8),	1.35(2)	1.37(2)	1.814(7)			
d		2.019(8), 2.08(1)	1.38(2)	1.39(2)	1.80(1)	147.0(7), 140.5(7)		
b		1.854(7), 1.80(1)	1.33(2)	1.33(2)	1.854(7)	134.2(8),		
d		2.08(1), 2.019(8)	1.38(2)	1.39(2)	1.80(1)	145(1)		
b		1.814(7)	1.37(1)	1.35(1)	1.836(8)	127.8(7), 124.5(9), 145(1)		
b		1.807(9)	1.38(2)	1.38(2)	1.807(9)	146.8(2)		
60e	Cu^{II}	2.375(1)	1.382(2)	1.376(2)	---	109.22(9)	R1=G1	(Zhang, et al., 2009)
61e	Cu^{II}	2.653(3), 2.547(3)	1.216(5) 1.219(4)	1.217(4) 1.218(5)	---	106.7(2), 112.1(2)	R1=tBu R3=G9 G2=G4=H	(Philibert, et al., 2003)
62f	Cu^{II}	2.359(2)	1.382(3)	1.382(3)	---	108.6(1)	R1= R2= G1, R3=R4=H	(Stylianou, et al., 2008)
63c	Ti^{IV}	2.048(3)	1.373(7)	1.371(6)	---	126.8(3)	R1=G12 R2-R3=R4=H	(Vaid, et al., 1999)
g		1.782(3)	1.387(6)	1.361(6)	2.208(4)	173.0(3),	R1=R2=R3=R4=H	(Vaid, et al.,

		1.782(3)	1.387(6)	1.361(6)	2.208(4)	125.9(3) 173.0(3), 125.9(3)		1999)
[b]		1.794(4)	1.376(7)	1.351(6)	1.923(3)	164.1(5), 129.3(3)	R1=R2=R3=R4=H	(Vaid, et al., 1999)
64[h]	Cu^{II}	1.921(2), 1.908(2)	1.403(8)	1.4025(8)	1.921(2), 1.908(2)	128.76(6), 125.70(6), 128.76(6), 125.70(6),	R1= R2= G14, R3= R4= H	(Phan, et al., 2011)
66[h]	Cu^{II}	1.931(7), 2.338(6)	1.36(1)	1.34(1)	1.920(7), 2.343(6)	116.2(5), 124.1(5),	R1= R2= G14, R3= R4= H	(Phan, et al., 2011)
67[h]	Zn^{II}	2.00(2)	1.36(3)	1.36(3)	2.00(2)	128(1), 130(1)	R1= R2= G6, R3=R4=H	(Dietzel, et al., 2008)
68[h]	Zn^{II}	1.96(1), 1.99(2)	1.38(3)	1.38(3)	1.96(1), 1.99(2)	125(1), 129(1)	R1= R2= G6, R3=R4=H	(Dietzel, et al., 2008)
69[h]	Cu^{II}	1.922(4), 2.514(4)	1.350(6)	1.350(6)	1.922(4), 2.514(4)	124.6(3), 113.6(3)	R1= R2= G14, R3=R4=H	(Kretz, et al., 2006)
70[a]	Zn^{II}	2.222(6)	1.233(9)	1.242(9)	---	135.7(5)	R_1= G23, R_2= R_3= CH_3, R_4= H	(Senge, et al., 1999)
71[b]	Rh^{II}	2.25(1)	1.24(2)	1.24(2)	2.25(1)	136.8(8)	R_1= R_2= CH_3, R_3= R_4= H	(Handa, et al., 1996)
72[b]	Mo^{II}	2.619(9)	1.28()	1.28(2)	2.594(9)	152.7(8), 141.7(8)	R_1= R_3= CH_3, R_2= R_4= H	(Handa, et al., 1995)
73[a]	Mo^{II}	2.569(6)	1.21(1)	1.24(1)	---	140.6(5)	R_1= R_3= tBu, R_2= R_4= H	(Handa, et al., 1995)

Table 1. Summary of structurally characterized hydroquinone/*p*-semiquinone/*p*-quinone transition metal complexes. Some important crystallographic data are also included. Abbreviations are according to figures 2 and 3. [a] Mode I, [b] mode II, [c] mode III, [d] mode IV, [e] mode V, [f] mode VI, [g] mode VII, [h] mode VIII according to figure 2

2.1 Simple hydroquinones

The first crystallographic report on a transition metal hydroquinone appeared in 1982 (Heistand, et al., 1982). Heistand et.al reported the structure of a binuclear iron(III) complex containing two iron-salen units bridged together with a simple deprotonated hydroquinone (coordination mode **II**, figure 4). Although the C-$O_{hydroquinonate}$ bond length [1.349(3) Å] is shorter than the C-O bond of free hydroquinone (1.398 Å), it is within the limits expected for this *p*-dioxolene's oxidation state. It is worth noticing here that the respective catecholate complex found in the crystal structure is ligated with Fe^{III} in a monodentate fashion, in contrast to the hydroquinone complex which even in 50 fold excess of $[Fe(salen)]^+$ crystallizes as dimer. Heistand et al. have assigned the formation of the dimer to the crystallization process. However, the fist coordination of Fe^{III} to *p*-hydroquinone enhances the acidity of the second OH, and this may account for the stabilization of the dinuclear complex. In contrast, the intra molecular H-bond stabilization in catechols reduces the acidity of the second OH favoring the formation of the mononuclear complex. Nevertheless, this is the first example showing that hydroquinone can function as bridging ligand.

Other examples of dinuclear complexes following a mode II coordination have been reported with simple hydroquinone to bridge two $Zr(acac)_3^+$ (**33**) (Evans, et al., 1998), or Fe^{III}(5,10,15,20-tetraphenylporphyrinato)$^+$ (**45**) (Rheingold & Miller, 2003), or $Ti^{IV}Cl(CP^*)_2^+$ (**38**) (Kunzel, et al., 1996), or $Ti^{III}(CP^*)_2$ (**37**) (Horacek, et al., 2010) or $W^{V}OCl$[hydrogen

tris(3,5-dimethylpyrazolyl)borate]$^{+}$ (**17**) (Stobie, et al., 2003) or $Mo^{V}OCl$[hydrogen tris(3,5-dimethylpyrazolyl)borate]$^{+}$ (**41**) (Ung, et al., 1996). The last two moieties present additional interest because they form trinuclear complexes with two hydroquinones bridging three of these groups in an open structure (**46**) (Ung, et al., 1999) or three hydroquinones bridging three groups in a close triangular structure (**42**) (**35**) (McQuillan, et al., 1998; McQuillan, et al., 1996) (Figure 5). The C-$O_{hydroquinonate}$ bond distances range from 1.320 up to 1.394 Å indicative of the hydroquinone oxidation state of the ligand.

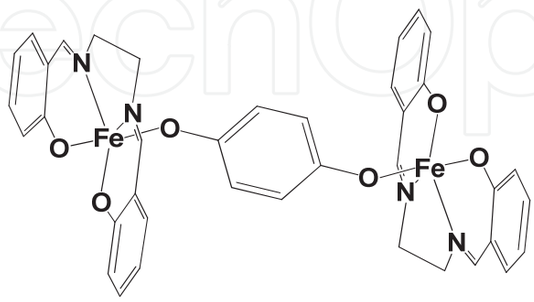

Fig. 4. Drawing of the molecular structure of first bridged hydroquinone complex **19**. The numbering of complexes is according to table 1

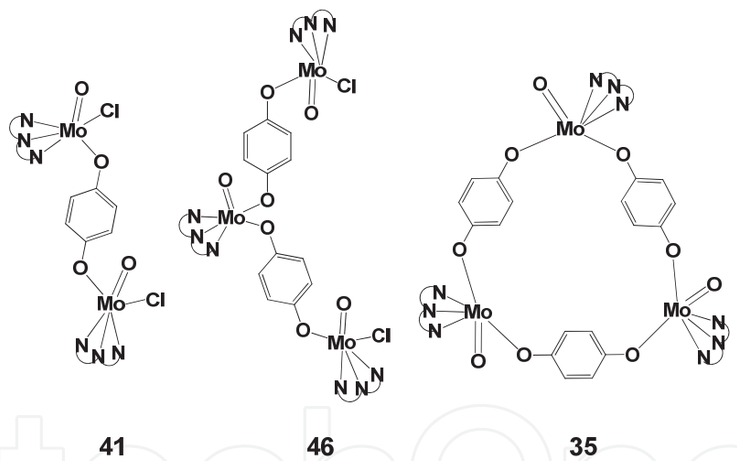

41 **46** **35**

Fig. 5. Drawings of the structure of the **41** monuclear, **46** trinuclear open structure, and **35** trinuclear trigonal structure, complexes of hydroquinone with $Mo^{V}OCl$[hydrogen tris(3,5-dimethylpyrazolyl)borate]$^{+}$ group. The numbering of complexes is according to table 1

In exploiting the bridging properties of hydroquinone, polymeric complexes of $Ti^{III/IV}$ and $V^{III/IV}$ have been synthesized and structurally characterized. The successful synthesis of polymeric architectures is based on the use of non chelating monodentate co-ligands, such as pyridine, which leave several positions open for coordination of the metal ion from hydroquinone. The crystal structures of these compounds show the hydroquinone to ligate metal ions in various bridging modes including, mode **II** (**32**), (**34**), (**31**) (Tanski, et al., 2000; Tanski & Wolczanski, 2001; Vaid, et al., 1997), mode **IV** (**63**) (Vaid, et al., 1997) and mode **VIII** (**51**) (Vaid, et al., 1997). A noticeable feature of these structures is the dependence of the M-$O_{hydroquinonate}$ bond distances on the coordination mode. For example, for the coordination

mode **II** the Ti-$O_{hydroquinonate}$ bond distance ranges from 1.782 up to 1.923 Å, which are shorter than the distances of the bridged Ti - μ-$O_{hydroquinonate}$ – Ti (2.042, 2.048 Å) and the Ti-$OH_{hydroquinonate}$ distance (2.207 Å). The crystal packing of these structures reveal the formation of 1D (**31**) (Tanski & Wolczanski, 2001), 2D (**34**) (Tanski, et al., 2000) and 3D polymers (**32**), (**63**) (Vaid, et al., 1997; Vaid, et al., 1999). The formation of lower dimension 1D polymers for the V^{IV} complex compared with the titanium ones, is mainly due to the less available positions for hydroquinone coordination (two for the vanadium and four for the titanium complexes) because of the presence of the V=O_{oxo} group and the smaller coordination number (5).
Structural characterized complexes with simple hydroquinone to ligate metal ions in monodentate manner (mode **I**) are very rare (table 1). Very interesting examples are the 3D hydrogen bonded structures of the homoleptic six coordinated tungsten complex [W(4-hydrophenoxy)$_6$] (**14**). (Vaid, et al., 2001)

2.2 Substituted hydroquinones

The substituted hydroquinones with chelate groups can be separated into two main categories, the 2- monosubstituted and the 2,5- bisubstituted.
Monosubstituted hydroquinones result in the formation of type **I**, **III**, or **VI** complexes (figure 2). The structure of the complex seems to be controlled from the metal and the substitution. In general, larger substitutions with groups that can form more chelate rings favor the monodentate coordination mode **I** and smaller groups tend to form binuclear M - μ-$O_{hydroquinonate}$ – M bridged type **III** complexes. An example, are the Cu^{II} complexes of the Schiff pyridine complexes **56** and **11** shown in figure 6. (Li, et al., 2000)

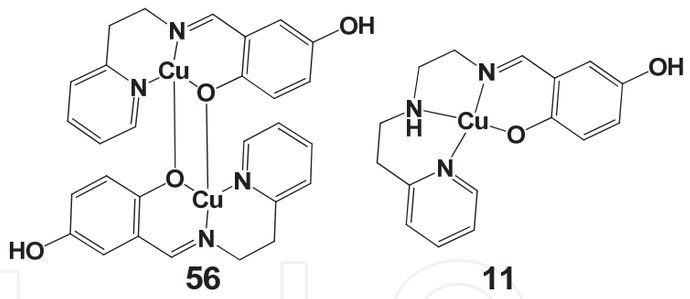

Fig. 6. Drawings of the structures of complexes **56** and **11** showing the effect of the size of the chelate group in the preference to type **III** and type **I** coordination modes respectively. The numbering of complexes is according to table 1

The Cu-$O_{hydroquinonate}$ bond distance of **11** (1.870 Å) is sufficiently shorter than the respective distances of **56** (1.932 – 1.976 Å) as expected. The C-$O_{hydroquinonate}$ bond distance of the ligated to the metal oxygen (1.321 and 1.350 Å) is also shorter than the free C-$OH_{hydroquinonate}$ bond (1.384 and 1.389 Å).
The protonated **VI** and the deproronated **I**, **III** of a complex are possible to be present in the solution of the reaction mixture and are dependent on the acidity-basicity of the solution. The speciation of water soluble complexes is controlled by pH and thus, various structural different complexes can be isolated. (Stylianou, et al., 2008) An example of the structures of the iminodiacetate monosubstituted hydroquinones isolated at different pHs are shown in figure 7.

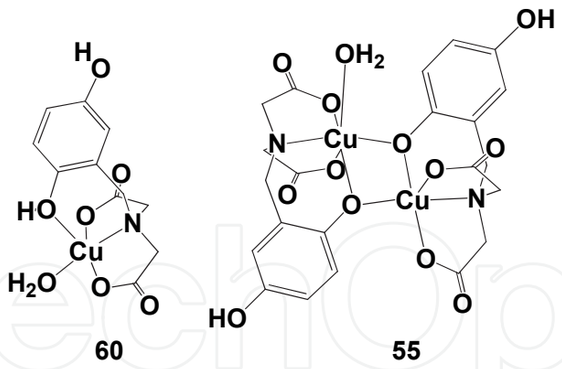

Fig. 7. Drawings of the structures of complexes **60** and **55** isolated from acidic and alkaline pHs respectively. (Stylianou, et al., 2008; Zhang, et al., 2009) The numbering of complexes is according to table 1

The $Cu^{II}_2O_2$ phenolate is a rare example of an asymmetric bridging core containing two copper atoms, one having a square pyramidal and the other an octahedral coordination sphere. This is the second example reported in the literature of the asymmetric $Cu^{II}_2O_2$ phenolate bridged complexes with the two copper ions exhibiting different coordination geometry (octahedral and square pyramidal). It is worth noticing here that although the type **III** dinuclear always crystallizes out of the alkaline solution, speciation studies have shown that the major species in solution is the type **I** mononuclear species. (Stylianou, et al., 2010)

Bisubstituted hydroquinones with chelate groups have been found to form with metal ions type **II**, **V** and **VII** structures. The same principles that we discussed for monosubstituted complexes are valid here too. However, the bisubstituted hydroquinone is a bridging ligand and chelate groups that leave the metal ion unsaturated lead to polymerization through additional coordination (for example complex **18**) (Dinnebier, et al., 2002) or through M-$O_{hydroquinonate}$-M bridging (for example complex **69**) (Kretz, et al., 2006)(figure 8).

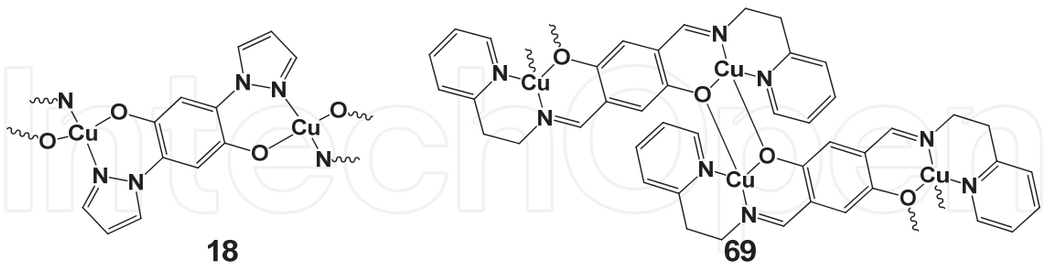

Fig. 8. Drawings of the polymeric structures of **18** and **69**. The numbering of complexes is according to table 1

Two very interesting examples of coordination modes **VII** and **V** are the structures of the complexes **62** and **55** (figure 9). In both complexes Cu^{II} ions are ligated to the same ligand (H_6bicah, figure 10), but they have been isolated from acidic and basic pHs respectively. Despite the fact that the hydroquinonate oxygen atom is deprotonated, the bond distances from Cu^{II} are very long [2.370(2) Å, 2.464(4) Å]. Deprotonation of the distant Y495 tyrosine in galactose oxidase accompanied with the strengthening of the interaction with copper ion

has been proposed to be an important step in the catalytic activity of the enzyme. In this structure, despite the deprotonation of the hydroquinone, the oxygen atom remains in axial position and therefore could be considered as an intermediate of this process.

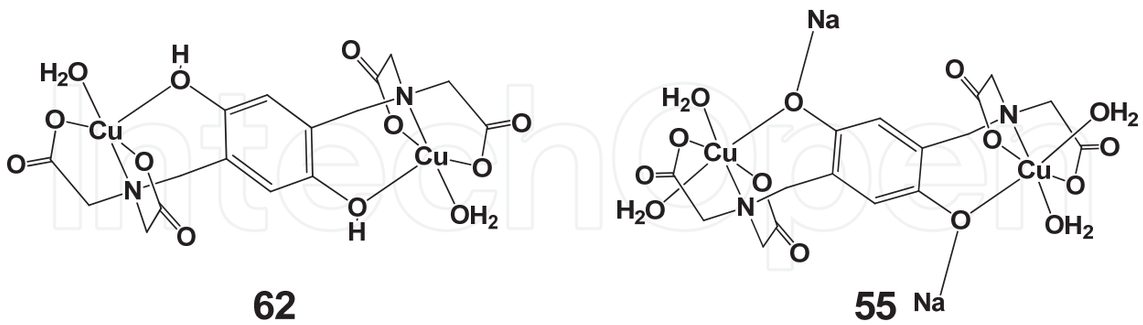

Fig. 9. Drawings of the structure of **62** and **55**. The numbering of complexes is according to table 1

2.3 Semiquinonates

There are only three *p*-semiquinonate complexes characterized by X-ray crystallography, and in all cases the semiquinone ligand bridges two V^{IV} ions. The ligands which are used for the stabilization of the semiquinone radicals are shown in figure 10.

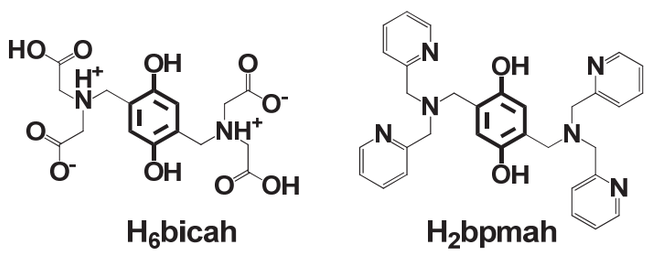

Fig. 10. 2,5- substituted iminodiacetic (**H_6bicah**) and bis(2-methylpyridyl)amine (**H_2bpmah**) hydroquinone ligands

The two of the three complexes have a rectangular shape structure, similarly to complexes **27, 28**: one has all vanadium atoms in oxidation state IV and both ligands in semiquinonate oxidation state (**15, 78**) and the other has two V^{IV} and two V^{V} ions ligated to a semiquinone and a hydroquinone ligand respectively (**29, 30**). The third complex is a V^{IV} dinuclear semiquinonate complex (**75, 79**) (figure 11). In addition to these compounds, the structures of the complexes with the ligands in hydroquinone oxidation state and the vanadium ions in IV or V or IV/V have been solved (figure 11). Because the structures of the complexes remain the same independently of the oxidation state of the ligand or the metal ion, this study gives us the opportunity for direct comparison between the compounds X-ray data.

The C-$O_{semiquinonate}$ bond distance ranges between 1.294 and 1.322 Å which is significantly shorter than the respective C-$O_{hydroquinonate}$ bond distance (1.328-1.366 Å) and designates the oxidation state of the ligand. The V^{IV}-$O_{semiquinonate}$ bond distances are significantly shorter than the respective V^{IV}-$O_{hydroquinonate}$ when complexes of the same ligand are compared. The mean values of the V^{IV}-$O_{semiquinonate}$ bond distances (1.89 ± 0.03 Å) calculated for all

complexes are also smaller than the mean values of V^{IV}-$O_{hydroquinonate}$ (1.94 ± 0.03 Å). Apparently, V^{IV} ions have higher affinity to bind the semiquinone oxygen atom than the hydroquinone and thus the ligation of V^{IV} is the main factor for stabilization of semiquinone radical in these complexes. More information about the affinity of the V^{IV} ion for the semiquinonate oxygen is being obtained from the C-$O_{hydroquinonate/semiquinonate}$-V angle. The C-$O_{semiquinonate}$-$V^{IV}$ angle (~137 °) is similar to the angle of C-$O_{hydroquinonate}$-V^{V} and indicates that the V^{IV}-$O_{semiquinonate}$ bond has significant π character. In contrast, the C-$O_{hydroquinonate}$-V^{IV} angle (~127 °) is significantly smaller, reflecting the weaker bonding between V^{IV} and $O_{hydroquinonate}$. However, the most interesting differences appear in the mixed oxidation ligand tetranuclear complexes **29** and **30** where the differences between the C-$O_{semiquinonate}$-V^{IV} and the C-$O_{hydroquinonate}$-V^{V} angles can be compared directly in the same molecule (Table 2). In these complexes the C-$O_{semiquinonate}$-V^{IV} angles (136.4 – 138.1 °) are significantly larger than the C-$O_{hydroquinonate}$-V^{V} (131.8-134.8 °), revealing that V^{IV}-$O_{semiquinonate}$ π bonding is stronger even than V^{V}-$O_{hydroquinonate}$.

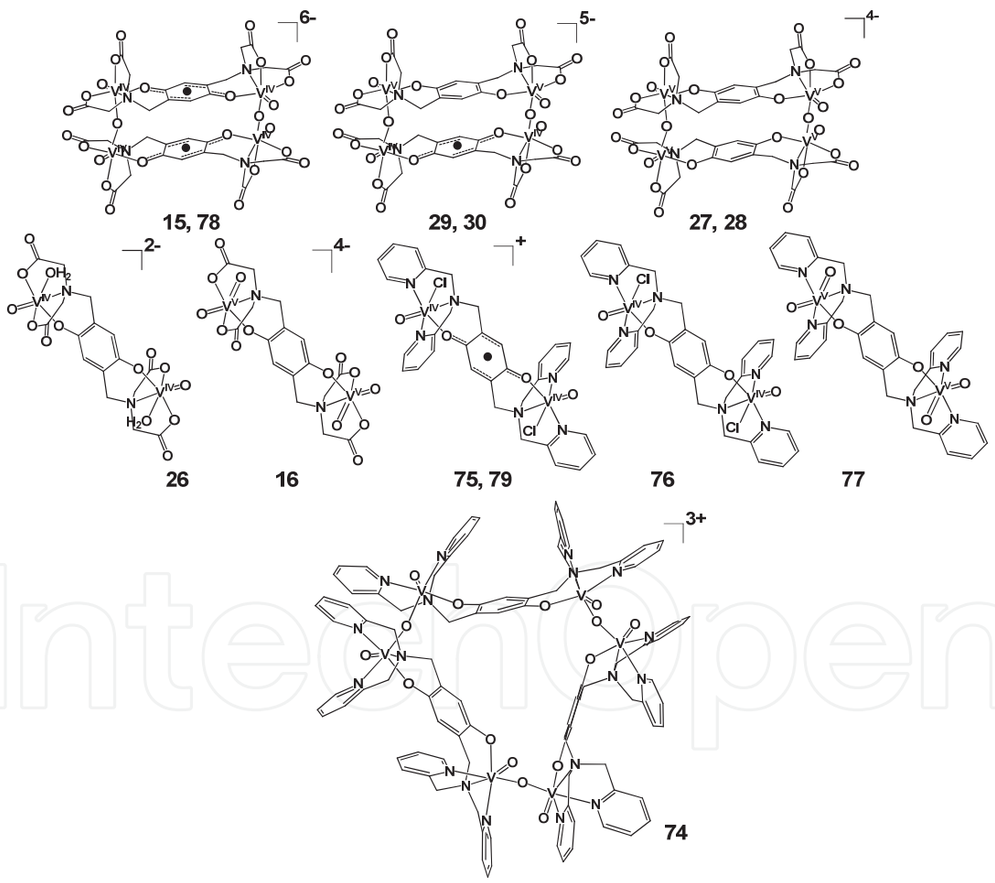

Fig. 11. Structures of vanadium complexes: 15, 16, 26-30, 74-79

2.4 *p*-Quinones

Complexes of *p*-quinones with transition metal ions are also rare. The quinone oxygen is a poor electron donor and thus, does not form easily σ- bonded complexes with transition

metal ions. A few examples that have been included in Table 1 show quinone to form complexes with soft metal centers. The most peculiar feature of these structures is that coordination of the $O_{quinone}$ causes elongation of the bond in comparison with the free quinone which is opposite to what is observed for the hydroquinones. For example, in the type **I** complex **70** the $C=O_{quinone}$ of the ligated oxygen is 1.242 Å, which is 0.09 Å larger than the length of $C=O_{quinone}$ of the free oxygen atom (Senge, et al., 1999). This lengthening shows that there is a significant π-back donation.

3. Charge distribution

One of the main perspective for developing the transition metal coordination chemistry of ligands derived from hydroquinone/*p*-semiquinone/quinone is associated with their rich redox activity and the potential of forming compounds that may exist in a number of electronic states due to the combined electrochemical activity of the metal ion and one or more quinone ligands (Drouza & Keramidas, 2007). Structural studies on X-ray crystallography has proven to be a valuable tool in the determination of charge distribution and delocalization in the coupling redox active metal ions and ligands. The *p*-dioxolene transition metal complexes have shown that the delocalization is not important.

3.1 Charge calculations based on the C-O and the intraring bond lengths

The C-O and the C-C intraring bond lengths of the *p*-dioxolene ligands are strongly dependent on the formal charge of the ligands (Drouza & Keramidas, 2007). The C-O distance exhibits the largest differences in the three oxidation states, ~1.35 Å in hydroquinone, ~1.32 Å in *p*-semiquinone and 1.24 Å in *p*-quinone and therefore, can be used for the assignment of the oxidation state of the ligand (table 1). In addition, the C-C interatomic bond distances are almost indistinguishable in hydroquinone ring (~1.40 Å), but they exhibit a long-short-long pattern in *p*-semiquinones (~ 1.42, ~ 1.37 and ~ 1.42 Å) which becomes more distinct in *p*-quinones (~ 1.46, ~ 1.33 and ~ 1.46 Å).

A quantitative approach in the evaluation of quinones charge is the linear relationship of the charge of dioxolenes (D) versus the C-O and all the six intraring C/C distances of the ligand, given by the equations 1 and 2; where d_i is the experimental *i*th bond length, and d_{1i} and d_{2i} are the *i*th bond lengths of the pure forms of catecholate and *o*-benzoquinone respectively.

$$\Delta_i = -2(d_i - d_{2i})/(d_{1i} - d_{2i}) \quad (1)$$

$$\Delta = (\Sigma w_i \Delta_i)/(\Sigma w_i) \quad (2)$$

This equation has been primarily used for the *o*-dioxolenes by Carugo et.al (Carugo, et al., 1992). Recently, these equations have been applied on the determination of the charge of *p*-dioxolenes using the bond lengths of a large number of ligands ligated to various metal ions (Drouza & Keramidas, 2007). The values of d_{1i} and d_{2i} for hydroquinone and *p*-quinones respectively are considered as the experimental bond lengths of the uncomplexed organic molecules. The ideal values of Δ are 0, -1 and -2 for Q, SQ and HQ respectively. The application of equations 1 and 2 on these bond lengths for all the complexes afforded Δ values that were statistical significant, matching the expected hydroquinonate, semiquinonate or quinone nature of *p*-dioxolenes ligated either to one or to two metal ions.

Important crystallographic data, calculation of the oxidation state of the metal ions using bond valence sums (BVS) and application of Δ calculations on the vanadium complexes of figure 11 are summarized in table 2. The results from these calculations confirm the oxidation states of the metal ions and the organic redox centers. Δ values deviate from the ideal values, with the largest deviation to be observed in one of the hydroquinones of complex **5**, (Δ = -1.56 instead of -2). These deviations are probably due to the coordination of the metal ion to the ligand and to the ionic or dipolar interactions of the complex with the counter ions and solvent molecules, which transfer charge from the organic ligands, thus distorting further the structures of *p*-dioxolenes. Despite these deviations the prediction of the organic ligand oxidation state has been successful and is in agreement with the oxidation state found from other spectroscopic techniques.

Comp.	V=O/Å	V–$O_{HQ/SQ}$ / Å	V-O_{bridge} / Å	C–$O_{HQ/SQ}$/ Å	C-$O_{HQ/SQ}$-V / deg	Δ	BVS ($V^{IV/V}$)
H_2bpmah				1.366(1)		–1.88, HQ	
75	1.598(2)	1.913(2)		1.294(3)	135.3(2)	–0.97, SQ	+4.14 (V^{IV})
76	1.606(2)	1.941(1)		1.329(2)	126.8(1)	–1.67, HQ	+3.92 (V^{IV})
	1.613(2)	1.938(2)		1.345(4)	127.5(2)	–1.77, HQ	+3.90 (V^{IV})
79	1.605(2)	1.914(2)		1.300(3)	134.8(1)	–1.13, SQ	+4.08 (V^{IV})
77	1.645(3)	1.903(2)	1.630(3)	1.345(4)	131.6(2)	–1.61, HQ	+4.98 (V^{V})
74	1.597(4)	1.854(3)	1.720(3)	1.360(5)	136.7(6)	–1.71, HQ	+5.11 (V^{V})
	1.593(3)	1.905(3)	1.843(3)	1.329(5)	128.4(7)		+4.35 (V^{IV})
	1.599(3)	1.940(3)	1.899(3)	1.330(5)	127.2(6)	–1.84, HQ	+4.19 (V^{IV})
	1.598(3)	1.844(3)	1.736(3)	1.343(6)	134.0(6)		+5.04 (V^{V})
	1.589(4)	1.925(4)	1.886(3)	1.369(6)	126.3(6)	–1.71, HQ	+4.28 (V^{IV})
	1.599(3)	1.848(4)	1.774(3)	1.352(6)	136.5(6)		+4.99 (V^{V})
26	1.601(3)	1.950(3)	2.002(3)	1.366(5)	124.8(3)	–1.94, HQ	+3.93 (V^{IV})
	1.606(3)	1.952(3)	2.009(3)	1.353(5)	128.2(2)	–1.85, HQ	+3.92 (V^{IV})
27	1.603(2)	1.824(1)	1.840(2)	1.338(2)	137.0(1)	–1.67, HQ	+5.03 (V^{V})
	1.610(2)	1.866(1)	1.748(2)	1.346(2)	132.3(1)		+5.05 (V^{V})
28	1.599(2)	1.827(2)	1.818(2)	1.335(3)	133.8(2)	–1.75, HQ	+5.10 (V^{V})
	1.620(2)	1.865(2)	1.729(2)	1.346(3)	132.3(2)		+5.07 (V^{V})
	1.606(2)	1.825(2)	1.875(2)	1.327(3)	137.2(2)	–1.56, HQ	+4.97 (V^{V})
	1.613(2)	1.878(2)	1.759(2)	1.325(3)	135.9(2)		+5.07 (V^{V})
29	1.622(2)	1.878(2)	1.697(2)	1.346(3)	134.8(2)	–1.72, HQ	+5.12 (V^{V})
	1.625(2)	1.879(2)	1.699(2)	1.352(3)	131.8(2)		+5.06 (V^{V})
	1.597(2)	1.880(2)	1.914(2)	1.312(3)	138.1(2)	–1.30, SQ	+4.24 (V^{IV})
	1.604(2)	1.936(2)	1.934(2)	1.309(3)	136.4(2)		+4.07 (V^{IV})
30	1.611(3)	1.885(2)	1.707(3)	1.348(4)	134.2(2)	–1.70, HQ	+5.11 (V^{V})
	1.630(2)	1.851(2)	1.699(2)	1.335(4)	134.8(2)		+5.11 (V^{V})
	1.609(2)	1.915(2)	1.926(2)	1.299(4)	137.2(2)	–1.24, SQ	+4.18 (V^{IV})
	1.607(3)	1.903(2)	1.915(3)	1.293(4)	137.1(2)		+4.20 (V^{IV})
78	1.616(2)	1.867(2)	1.813(2)	1.321(3)	135.2(2)	–1.38, SQ	+4.40 (V^{IV})
	1.618(2)	1.879(2)	1.809(2)	1.313(3)	136.4(2)		+4.42 (V^{IV})
15	1.620(3)	1.886(3)	1.807(1)	1.322(5)	137.0(3)	-1.39, SQ	+4.35 (V^{IV})
16	1.652(3)	1.864(3)	1.620(4)	1.354(5)	131.6(3)	-2.02, HQ	+5.22 (V^{V})
	1.641(4)	1.878(3)	1.626(4)	1.353(6)	131.9(3)	-1.95, HQ	+5.22 (V^{V})

Table 2. Comparison of Selected Chemical Bonds, and Δ Values for ligand, Binuclear $V^{IV/V}$ and Hexanuclear V^{IV} Complexes Respectively

3.2 Graphical discrimination of *p*-dioxolenes oxidation state

A nice graphical overview of the dependence of the C-$O_{Hydroquinonate/Semiquinonate}$ and V-$O_{Hydroquinonate/Semiquinonate}$ bond lengths, C-$O_{Hydroquinonate/Semiquinonate}$-V angle and Δ on the oxidation state of vanadium ion and the *p*-dioxolene ligand for the vanadium complexes contained in Table 2 is shown in figure 12.

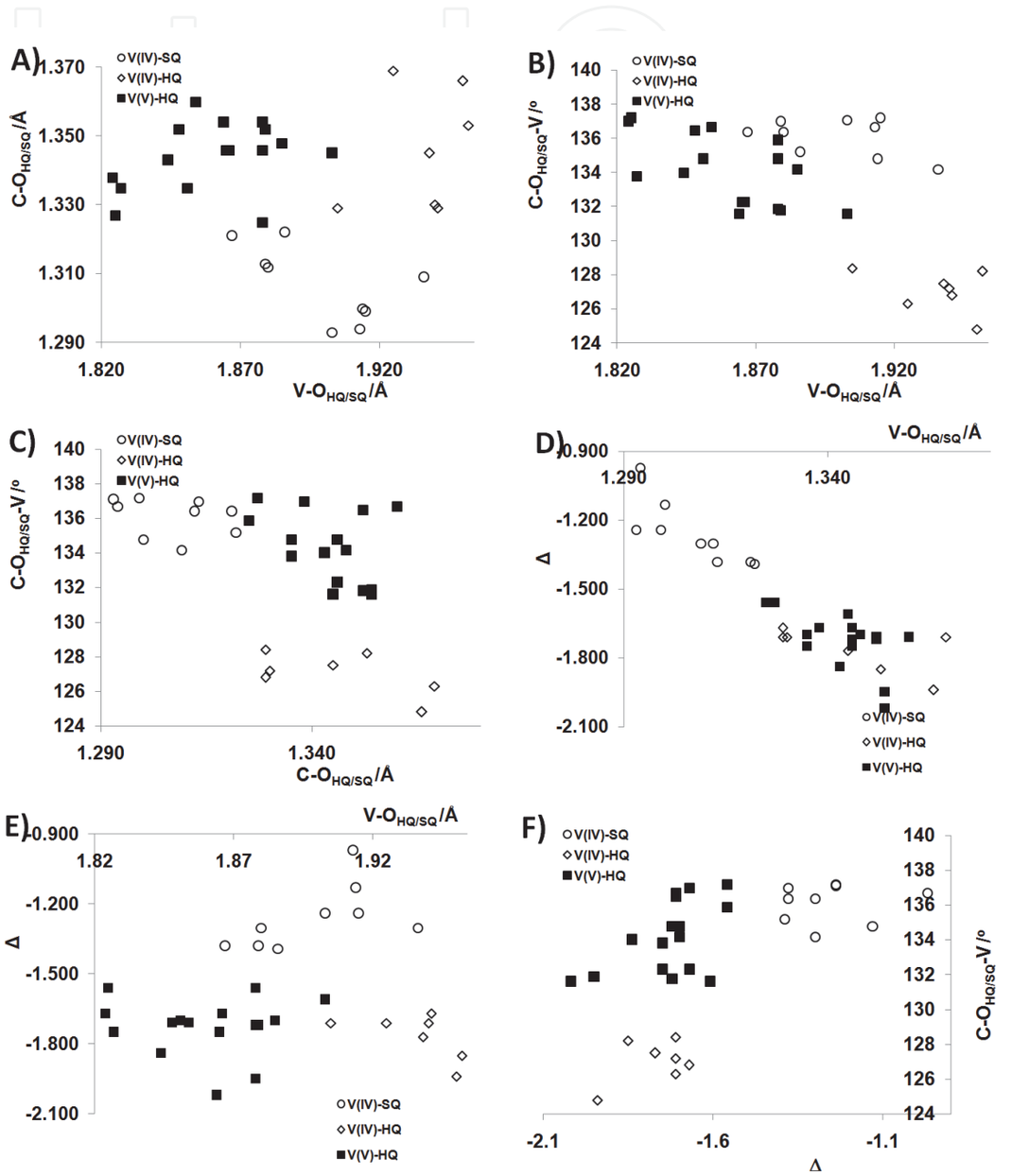

Fig. 12. Graphical presentations of the dependence of the C-$O_{HQ/SQ}$ / V-$O_{HQ/SQ}$ bond lengths, C-$O_{HQ/SQ}$-V and Δ/V-$O_{HQ/SQ}$ over the oxidation state of vanadium ion and the *p*-dioxolene ligand for the vanadium complexes in figure 11. HQ=hydroquinone, SQ=Semiquinone

The graph of C-$O_{Hydroquinonate/Semiquinonate}$ / V-$O_{Hydroquinonate/Semiquinonate}$ (figure 12A) gives separate regions for the different metal ligand oxidation states, however some of the values are at the border lines, mainly because the respective V-$O_{Hydroquinonate/Semiquinonate}$ deviate from the expected average bond lengths. The graphs of the C-$O_{Hydroquinonate/Semiquinonate}$-V angle versus V-$O_{Hydroquinonate/Semiquinonate}$ and C-$O_{Hydroquinonate/Semiquinonate}$ (Figure 12B, 12C) separate better the ligands oxidation state. There is a poor separation between the V^{V}-Hydroquinonate and V^{IV}-Semiquinonate complexes in C-$O_{Hydroquinonate/Semiquinonate}$ -V/V-$O_{Hydroquinonate/Semiquinonate}$ graphs because of the similar lengths between V^{V}-$O_{Hydroquinonate}$ and V^{IV}-$O_{Semiquinonate}$ bond lenghts. On the other hand C-$O_{Hydroquinonate/Semiquinonate}$-V/C-$O_{Hydroquinonate/Semiquinonate}$ graph gives a better separation between the different oxidation states. Among the graphs of C-$O_{Hydroquinonate/Semiquinonate}$, V-$O_{Hydroquinonate/Semiquinonate}$ and C-$O_{Hydroquinonate/Semiquinonate}$-V versus Δ (Figure 12D, 12E, 12F) the latter gives the best redox discrimination. Concluding, Δ and C-$O_{Hydroquinonate/Semiquinonate}$-V angle are the best parameters for the differentiation of the ligands oxidation state and of the strong V-O bonded V^{V}-Hydroquinonate and V^{IV}-Semiquinonate compounds than the weaker V^{IV}-Hydroquinonate respectively.

4. Utilization of X-ray crystallography as a characterization tool for the development of functional bioinorganic models based on hydroquinone/*p*-semiquinone ligands

The study of the bioinorganic model compounds significantly contributes to: a) the investigation of metal ions mechanisms and reactivity in biological systems and b) the development of efficient and selective stable catalysts that will mimic the activity of the enzymes. For example, the development of metal-quinone complexes and stabilization of the radicals has been inspired mainly from two redox center metal-enzymes that use modified *p*-semiquinone and phenolic radicals to facilitate two electron reduction of O_2 to H_2O_2 with subsequent oxidation of an organic substrate. The O_2/H_2O_2 oxidative C-H activation by the transition metal bioinorganic-based complexes constitutes a very important industrial process. X-ray crystallography has proven to be an essential tool for the successful implementation of the targets of bioinorganic chemistry, in particular, in deciphering the complicated multivariate aqueous systems. Some applications of crystallography may include the gathering of information about the speciation of the complexes in aqueous solutions and the providing of evidence for the molecules reactivity. In this chapter, we will discuss our most recent work in the development of vanadium based hydroquinone/semiquinone model systems for the investigation of reduction of O_2 induced by the metal ions in acidic aqueous solutions.

4.1 $V^{V/IV}$-hydroquinone/semiquinone models compounds

The V^{IV} complexes with the modified-hydroquinones H_6bicah, H_2bpmah (figure 10), have some very interesting features: they are water soluble, they stabilize *p*-semiquinone radicals in acidic conditions and they reduce dioxygen. Apparently, these compounds function both as activators and as radical traps and thus provide important information for the investigation of O_2 activation reactions by the isolation of reactive intermediates.

The tetranuclear V^{IV} bicah^{6-} complexes (figure 11) exhibit a pH induced electron transfer from the metal center to the ligand and subsequent fast oxidation from the atmospheric

oxygen, in acidic pHs (4.5 – 3.0). (Drouza & Keramidas, 2008) As described above for this solution, the three tetranuclear complexes **15**, **29** and **27** (figure 11) were isolated and characterized by crystallography at pHs 4.5, 3.4 and 3.0 respectively. Based on these data a possible mechanism of a two step reaction of **15** has been proposed and is shown in figure 13. At the first step, an aqueous solution of **15** is acidified (pH=3.4), resulting in one electron transfer from one of the attached to semiquinones V^{IV} to the semiquinonate radical. The formed hydroquinone is immediately oxidized to semiquinone from the atmospheric oxygen and then the second V^{IV} is oxidized from the semiquinone to give **29**. At the second step, the semiquinone of the second dinuclear unit is also reduced, oxidizing one of the attached V^{IV} ions at pH=3.0 and proceeds to the formation of **27** following a similar mechanism. The trigger for this electron transfer, which finally results in oxidation of the complex from dioxygen, is the semiquinone protonation at acidic conditions. The mechanism is supported mainly by the isolation and the structural characterization of the initial and final products **15, 29, 27**, however none of the intermediates **id1-4** has been isolated or characterized. The reasons for not isolating the intermediates are a) the facile oxidation of the formed hydroquinone from the atmospheric oxygen and b) the almost overlapping redox potentials of the one electron $V^{V} \rightarrow V^{IV}$ and semiquinone→hydroquinone redox processes, and the structural similarity between the redox species which permits the fast electron transfer from the V^{IV} to the semiquinone radical.

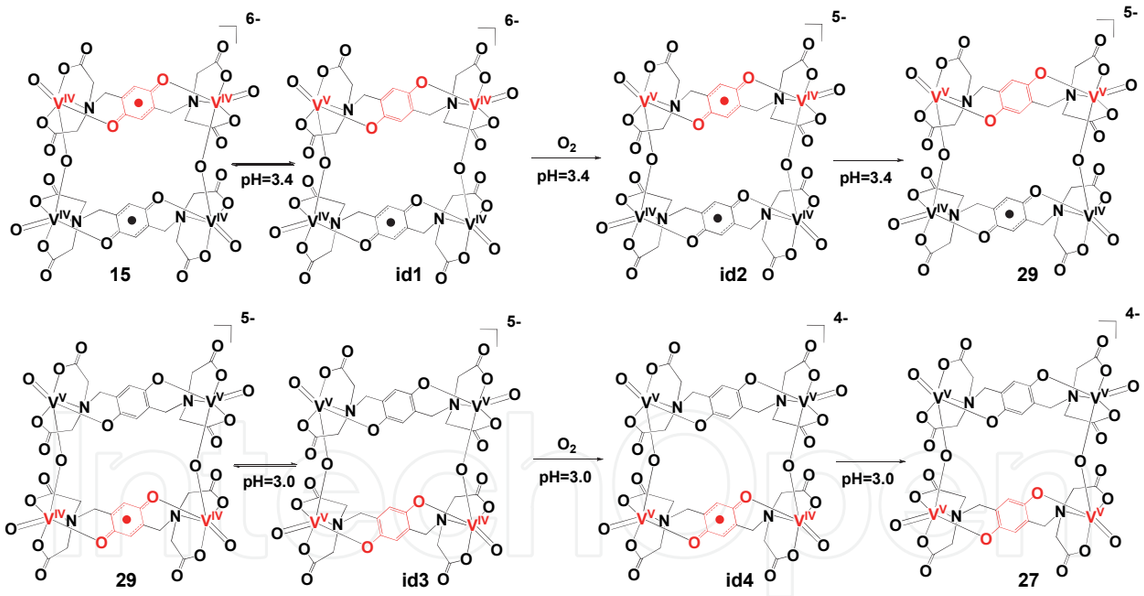

Fig. 13. Possible mechanism of the stepwise pH induced oxidation of the tetranuclear V^{IV}-semiquinonate complex **15**

Isolation and structural characterization of the intermediates will confirm our hypothesis, however the stabilization of these species is required. The strategy we followed (Stylianou, et al., 2011) was the stabilization of vanadium in oxidation state IV. This was achieved by the increase of the $V^{V} \rightarrow V^{IV}$ redox potential with the replacement of the hard oxygen carboxylate donor atoms ($bicah^{6-}$) with the softer pyridine nitrogen donor atoms ($bpmah^{2-}$) (figure 10). Thus, the respective $bpmah^{2-}$intermediate complexes will be trapped because this semiquinone is not strong enough to oxidize the stabilized V^{IV} to V^{V}.

Indeed, complex **76** is being oxidized in aqueous solutions in two steps, first oxidation of the organic ligand to semiquinone (complex **75**) at pH 2.8 and then transfer of an electron from V^{IV} to the semiquinone at pH 2.2 resulting in the formation of the hexanuclear complex **74** (figure 14).

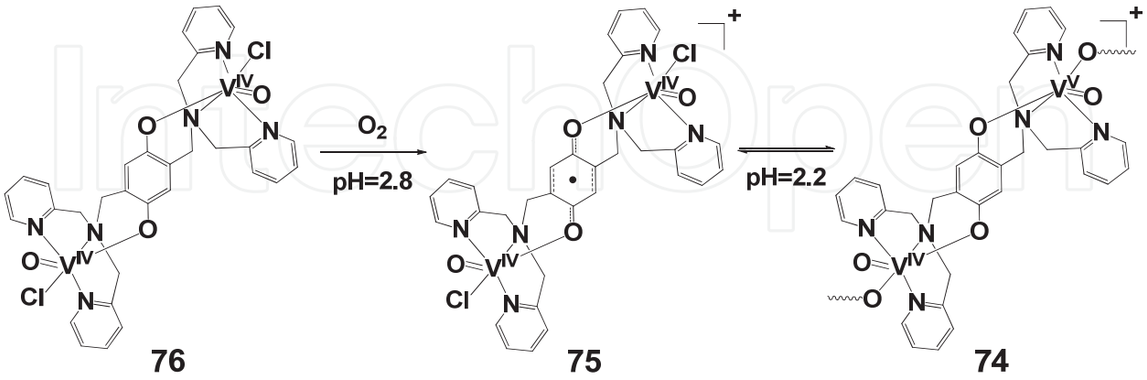

Fig. 14. Mechanism of the two step oxidation of **76** in aqueous solution

Although the $bpmah^{2-}$ complexes (two dinuclear oxo-bridged units) are structurally different from the respective compounds of $bicah^{6-}$ (one dinuclear unit), from the comparison of the reaction mechanism in figure 13 with this in figure 14, it is apparent that complex **76** is analogous to **id1**, **id3**, complex **75** to **id2**, **id4** and complex **74** to **29**, **27**. Complex **76** is stable in solution at pH 3.4, however, it is very rapidly oxidized to semiquinone radical at pH=2.8 from dioxygen. As we have predicted, the pyridine nitrogen donor atoms stabilize the oxidation state IV of vanadium. At pH 2.2 the oxophilicity of the metal increases, resulting in replacement of the chlorine with an oxo bridging group. This change of vanadium coordination environment is expected to reduce the $V^{IV} \rightarrow V^{V}$ redox potential and in combination with the stronger oxidative ability of semiquinone at lower pH (Baruah, et al., 2002; Drouza & Keramidas, 2008; Rath, et al., 1999) it results in electron transfer from V^{IV} to semiquinone and the slow formation of the V^{IV}/V^{V} mixed valent hydroquinone complex **74**.

Hydroquinone is not a strong reducing agent and thus cannot directly reduce O_2. It is certain that the interaction of the metal ion with O_2 increases the one electron reduction potential of dioxygen to superoxide radical oxidizing hydroquinone to semiquinone. Superoxide is further reduced to peroxide. One of the most surprising features of the semiquinone complex **75** is its low oxophilicity that increases at lower pH, as shown by the formation of **74**. Examples in the literature show that V^{IV} complexes with pyridine type donors are highly oxophilic, thus, it is probable that the bonding with the semiquinone radical softens the metal ion. This is important for further understanding the reactivity of vanadium at the oxidation reactions of organic substrates from the metal activated O_2. However, full understanding of the properties of these radical complexes requires more *p*-semiquinone complexes to be synthesized and crystallographically characterized. In detailed investigation of these mechanisms, the involvement of additional electrochemical, magnetic and spectroscopic techniques are required. However, crystallography is always the best way to start. It constitutes the first priority in the development of new bioinorganic model compounds.

5. Conclusions

The difficulties in the synthesis of stable transition metal – hydroquinone/semiquinone/ quinone complexes have delayed the development of this chemistry relative to the phenol and catechol ones. The notion that *p*-dioxolene chemistry resembles that of phenols or *o*-dioxolenes and thus the study of those molecules also covers hydroquinones is mistaken. *p*-Dioxolenes have different reactivity. They are more reactive than phenols and less reactive than *o*-dioxolenes. In addition, as it has been shown, it is a bridging ligand which provides functional polymeric materials with novel optical, redox and magnetic properties. The last ten years, the importance of these ligands in the synthesis of bioinorganic models, in the development of bioinspiring "green" catalysts and of functional materials has been recognized, resulting in an increase of the structurally characterized *p*-dioxolene transition metal complexes.

Here, we have reviewed the rich coordination chemistry of *p*-dioxolenes with transition metals found in their crystal structures, examined the structural data that can be applied for the calculation of ligand charge and understood the factors in the metal induced stabilization of *p*-semiquinone radicals. V^{IV} is the only ion found up to now to stabilize the σ-bonded *p*-semiquinone radical. The stabilization is a result of the very strong bond between the metal and the oxygen of the dioxolene ligand. These binary metal-organic redox bioinorganic models have rich pH induced redox chemistry in aqueous solution as it has been proven from the detailed crystallographic study of the species produced at various pHs. Particular impetus for future research aimed at these molecules is provided by the established significance in O_2 activation reactions.

The structural chemistry of *p*-dioxolenes transition metal complexes is to a large extent unexplored. However, the unique redox properties and structural diversity of these ligands in combination with the recent advances in novel syntheses for the stabilization of the complexes have attracted the scientific curiosity, and thus, a prosperous future for this chemistry is waiting to be seen.

6. Acknowledgment

We thank the Research Promotion Foundation of Cyprus and the European Structural Funds for the financial support of this work with the proposals ΔΙΔΑΚΤΩΡ/ΔΙΣΕΚ/0308/49.

7. References

Arévalo, S., Bonillo, M.R., de Jesús, E., de la Mata, F.J., Flores, J.C., Gómez, R., Gómez-Sal, P. & Ortega, P., (2003). Synthesis of polymetallic Group 4 complexes bridged by benzenediolate and triolate ligands. X-ray crystal structure of [{Ti(C5Me5)Cl2}2{[mu]-1,4-O(2,3-C6H2Me2)O---}]. *Journal of Organometallic Chemistry*, Vol.681, No.1-2, pp. 228-236, ISSN 0022-328X

Baruah, B., Das, S. & Chakravorty, A., (2002). A family of vanadate esters of monoionized and diionized aromatic 1,2-diols: Synthesis, structure, and redox activity. *Inorganic Chemistry*, Vol.41, No.17, pp. 4502-4508, ISSN 0020-1669

Becker, J.M., Barker, J., Clarkson, G.J., van Gorkum, R., Johal, G.K., Walton, R.I. & Scott, P., (2010). Chirality and diastereoselection in the mu-oxo diiron complexes L(2)Fe-O-

FeL(2) (L = bidentate salicylaldiminato). *Dalton Transactions*, Vol.39, No.9, pp. 2309-2326, ISSN 1477-9226

Berthon, R.A., Colbran, S.B. & Craig, D.C., (1992). Palladium(II) complexes of 2-(2,5-dimethoxyphenyl)-1,10-phenathrolinr (phenhqme2) and 2-(2,5-hydroquinonyl)-1,10-phenathroline (phenhqh2) - the x-ray crystal-structure of PDCL (phenhqh).H2O.(CH3)2SO. *Polyhedron*, Vol.11, No.2, (Jan), pp. 243-250, ISSN 0277-5387

Brandon, E.J., Rogers, R.D., Burkhart, B.M. & Miller, J.S., (1998). The structure and ferrimagnetic behavior of meso-tetraphenyl-porphinatomanganese(III) tetrachloro-1,4-benzoquinonide, (MnTPP)-T-III (+) QCl(4) (center dot-)center dot PhMe: Evidence of a quinoidal structure for QCl(4) (center dot-). *Chemistry-a European Journal*, Vol.4, No.10, (Oct), pp. 1938-1943, ISSN 0947-6539

Caldwell, S.L., Gilroy, J.B., Jain, R., Crawford, E., Patrick, B.O. & Hicks, R.G., (2008). Synthesis and redox properties of a phosphine-subsituted para-dioxolene and its bimetallic palladium complex. *Canadian Journal of Chemistry-Revue Canadienne De Chimie*, Vol.86, No.10, (Oct), pp. 976-981, ISSN 0008-4042

Calvo, R., Abresch, E.C., Bittl, R., Feher, G., Hofbauer, W., Isaacson, R.A., Lubitz, W., Okamura, M.Y. & Paddock, M.L., (2000). EPR study of the molecular and electronic structure of the semiquinone biradical Q(A)(-center dot) Q(B)(-center dot) in photosynthetic reaction centers from Rhodobacter sphaeroides. *Journal of the American Chemical Society*, Vol.122, No.30, (Aug), pp. 7327-7341, ISSN 0002-7863

Carugo, O., Castellani, C.B., Djinović, K. & Rizzi, M., (1992). Ligands derived from o-benzoquinone: Statistical correlation between oxidation state and structural features. *Journal of the Chemical Society, Dalton Transactions*, No.5, pp. 837-841, ISSN 0300-9246

Dietzel, P.D.C., Johnsen, R.E., Blom, R. & Fjellvag, H., (2008). Structural changes and coordinatively unsaturated metal atoms on dehydration of honeycomb analogous microporous metal-organic frameworks. *Chemistry-a European Journal*, Vol.14, No.8, pp. 2389-2397, ISSN 0947-6539

Dinnebier, R., Lerner, H.W., Ding, L., Shankland, K., David, W.I.F., Stephens, P.W. & Wagner, M., (2002). One-dimensional spin chains from Cu-II ions and 2,5-bis(pyrazol-1-yl)-1,4-dihydroxybenzene. *Zeitschrift Fur Anorganische Und Allgemeine Chemie*, Vol.628, No.1, (Jan), pp. 310-314, ISSN 0044-2313

Drouza, C. & Keramidas, A.D. (2007). Charge distribution in vanadium p-(hydro/semi)quinonate complexes. In: *Vanadium: The Versatile Metal,* Kustin, K., et al (Ed.), pp.352-363, American Chemical Society, ISBN 9780841274464, Washington, DC

Drouza, C. & Keramidas, A.D., (2008). Solid state and aqueous solution characterization of rectangular tetranuclear V-IV/V-p-semiquinonate/hydroquinonate complexes exhibiting a proton induced electron transfer. *Inorganic Chemistry*, Vol.47, No.16, (Aug), pp. 7211-7224, ISSN 0020-1669

Drouza, C., Tolis, V., Gramlich, V., Raptopoulou, C., Terzis, A., Sigalas, M.P., Kabanos, T.A. & Keramidas, A.D., (2002). p-hydroquinone-metal compounds: synthesis and crystal structure of two novel V-V-p-hydroquinonate and V-IV-p-semiquinonate species. *Chemical Communications*, No.23, pp. 2786-2787, ISSN 1359-7345

Errington, R.J., Petkar, S.S., Middleton, P.S., McFarlane, W., Clegg, W., Coxall, R.A. & Harrington, R.W., (2007). Non-aqueous synthetic methodology for TiW5 polyoxometalates: protonolysis of (MeO) TiW5O18 (3-) with alcohols, water and phenols. *Dalton Transactions*, No.44, pp. 5211-5222, ISSN 1477-9226

Evangelio, E. & Ruiz-Molina, D., (2005). Valence tautomerism: New challenges for electroactive ligands. *European Journal of Inorganic Chemistry*, No.15, (Aug), pp. 2957-2971, ISSN 1434-1948

Evans, W.J., Ansari, M.A. & Ziller, J.W., (1998). The reactivity of zirconium acetylacetonate with phenols. *Polyhedron*, Vol.17, No.2-3, pp. 299-304, ISSN 0277-5387

Gelling, O.J., Meetsma, A. & Feringa, B.L., (1990). Bimetallic oxidation catalysts-synthesis, x-ray-analysis, and reactivity of a binuclear para-hydroquinone-containing copper(II) complex. *Inorganic Chemistry*, Vol.29, No.15, (Jul), pp. 2816-2822, ISSN 0020-1669

Handa, M., Matsumoto, H., Namura, T., Nagaoka, T., Kasuga, K., Mikuriya, M., Kotera, T. & Nukada, R., (1995). Chain and discrete dimer complexes of molybdenum(II) trifluoroacetate axially coordinated by p-quinones, Mo-2(O2CCF3)(4)(2,6-Me-BQ)(N) (2,6-Me-BQ=2,6-dimethyl-p-benzoquinone) and Mo-2(O2CCF3)(4)(2,6-t-Bu-BQ)(2) (2,6-t-Bu-BQ=2,6-di-t-Butyl-p-benzoquinone). *Chemistry Letters*, No.10, (Oct), pp. 903-904, ISSN 0366-7022

Handa, M., Mikuriya, M., Sato, Y., Kotera, T., Nukada, R., Yoshioka, D. & Kasuga, K., (1996). Chain compounds of rhodium(II) trifluoroacetate linked by p-quinone Rh-2(O2CCF3)(4)(p-Q) (n), p-Q=1,4-benzoquinone, 1,4-naphthoquinone, and 2,3-dimethyl-1,4-benzoquinone. *Bulletin of the Chemical Society of Japan*, Vol.69, No.12, (Dec), pp. 3483-3488, ISSN 0009-2673

He, Z.C., Colbran, S.B. & Craig, D.C., (2003). Could redox-switched binding of a redox-active ligand to a copper(II) centie drive a conformational proton pump gale? A synthetic model study. *Chemistry-a European Journal*, Vol.9, No.1, (Jan), pp. 116-129, ISSN 0947-6539

Heistand, R.H., Roe, A.L. & Que, L., (1982). Dioxygenase models - crystal - structures of N,N'-(1,2-phenylene)bis(salycyldeniminato)(catecholato-O)iron(III) and mu-(1,4-benzenediolato-O,O')-bis N,N'-ethylnebis(salicylideniminato)iron(III). *Inorganic Chemistry*, Vol.21, No.2, pp. 676-681, ISSN 0020-1669

Horacek, M., Gyepes, R., Cisarova, I., Kubista, J., Pinkas, J. & Mach, K., (2010). Synthesis and structure of dinuclear dimethylene- or 1,4-phenylene-linked bis(decamethyltitanoceneoxide) (Ti(III)) complexes. *Journal of Organometallic Chemistry*, Vol.695, No.21, (Oct), pp. 2338-2344, ISSN 0022-328X

Huang, F.P., Wang, Y.X., Zhao, J., Bian, H.D., Yu, Q. & Liang, H., (2008). p-hydroquinone-metal complex: Synthesis, crystal structure and electrochemical property. *Chinese Journal of Inorganic Chemistry*, Vol.24, No.9, (Sep), pp. 1523-1526, ISSN 1001-4861

Iwata, S., Lee, J.W., Okada, K., Lee, J.K., Iwata, M., Rasmussen, B., Link, T.A., Ramaswamy, S. & Jap, B.K., (1998). Complete structure of the 11-subunit bovine mitochondrial cytochrome bc(1) complex. *Science*, Vol.281, No.5373, (Jul), pp. 64-71, ISSN 0036-8075

Klinman, J.P., (1996). Mechanisms whereby mononuclear copper proteins functionalize organic substrates. *Chemical Reviews*, Vol.96, No.7, (Nov), pp. 2541-2561, ISSN 0009-2665

Kondo, M., Nabari, K., Horiba, T., Irie, Y., Kabir, M.K., Sarker, R.P., Shimizu, E., Shimizu, Y. & Fuwa, Y., (2003). Synthesis and crystal structure of Ni{bis(2,5-dihydroxysalicylidene)ethylenediaminato} : a hydrogen bonded assembly of Ni(II)-salen complex. *Inorganic Chemistry Communications*, Vol.6, No.2, (Feb), pp. 154-156, ISSN 1387-7003

Kretz, T., Bats, J.W., Losi, S., Wolf, B., Lerner, H.W., Lang, M., Zanello, P. & Wagner, M., (2006). Hydroquinone-bridged dinuclear CuII complexes and single-crystalline Cu-II coordination polymers. *Dalton Transactions*, No.41, pp. 4914-4921, ISSN 1477-9226

Kumbhakar, D., Sarkar, B., Maji, S., Mobin, S.M., Fiedler, J., Urbanos, F.A., Jimenez-Aparicio, R., Kaim, W. & Lahiri, G.K., (2008). Intramolecular Valence and Spin Interaction in meso and rac Diastereomers of a p-Quinonoid-Bridged Diruthenium Complex. *Journal of the American Chemical Society*, Vol.130, No.51, (Dec), pp. 17575-17583, ISSN 0002-7863

Kunzel, A., Sokolow, M., Liu, F.Q., Roesky, H.W., Noltemeyer, M., Schmidt, H.G. & Uson, I., (1996). Synthesis and characterisation of quinonide bridged dinuclear complexes of titanium and zirconium. *Journal of the Chemical Society-Dalton Transactions*, No.6, (Mar), pp. 913-919, ISSN 0300-9246

Li, P.Y., Solanki, N.K.I., Ehrenberg, H., Feeder, N., Davies, J.E., Rawson, J.M. & Halcrow, M.A., (2000). Copper(II) complexes of hydroquinone-containing Schiff bases. Towards a structural model for copper amine oxidases. *Journal of the Chemical Society-Dalton Transactions*, No.10, pp. 1559-1565, ISSN 0300-9246

Litos, C., Terzis, A., Raptopoulou, C., Rontoylanni, A. & Karaliota, A., (2006). Polynuclear oxomolybdenum(VI) complexes of dihydroxybenzoic acids: Synthesis, spectroscopic and structure characterization of a tetranuclear catecholato-type coordinated 2,3-dihydroxybenzoate and a novel tridentate salicylato-type coordinated 2,5-dihydroxybenzoate trinuclear complex. *Polyhedron*, Vol.25, No.6, (Apr), pp. 1337-1347, ISSN 0277-5387

Margraf, G., Bats, J.W. & Wagner, M., (2009). *Cambridge Structural Database* pp. ISSN

Margraf, G., Kretz, T., de Biani, F.F., Laschi, F., Losi, S., Zanello, P., Bats, J.W., Wolf, B., Removic-Langer, K., Lang, M., Prokofiev, A., Assmus, W., Lerner, H.W. & Wagner, M., (2006). Mono-, di-, and oligonuclear complexes of Cu-II ions and p-hydroquinone ligands: Syntheses, electrochemical properties, and magnetic Behavior. *Inorganic Chemistry*, Vol.45, No.3, (Feb), pp. 1277-1288, ISSN 0020-1669

Matalobos, J.S., Garcia-Deibe, A.M., Fondo, M., Navarro, D. & Bermejo, M.R., (2004). A di-mu-phenoxo bridged zinc dimer with unfamiliar spatial arrangement. *Inorganic Chemistry Communications*, Vol.7, No.2, (Feb), pp. 311-314, ISSN 1387-7003

McQuillan, F.S., Berridge, T.E., Chen, H.L., Hamor, T.A. & Jones, C.J., (1998). Bi-, tri-, and tetranuclear metallomacrocycles constructed by metal-directed reactions involving resorcinol or hydroquinone or by addition of octahedral metal centers to tetrahexylcalix 4 resorcinarene: X-ray crystal structure of syn,syn- Mo{HB(3,5-Me2C3HN2)(3)}(NO)(1,4-O2C6H4) (3). *Inorganic Chemistry*, Vol.37, No.19, (Sep), pp. 4959-4970, ISSN 0020-1669

McQuillan, F.S., Chen, H.G., Hamor, T.A. & Jones, C.J., (1996). Metal directed syntheses of metallocyclophanes containing triangular arrays of interacting redox active octahedral metal centres, X-ray crystal structure of W(Tp*)(NO)(OC6H4O) (3). *Polyhedron*, Vol.15, No.21, pp. 3909-3913, ISSN 0277-5387

Phan, N.H., Halasz, I., Opahle, I., Alig, E., Fink, L., Bats, J.W., Cong, P.T., Lerner, H.W., Sarkar, B., Wolf, B., Jeschke, H.O., Lang, M., Valenti, R., Dinnebier, R. & Wagner, M., (2011). Thermally induced crystal-to-crystal transformations accompanied by changes in the magnetic properties of a Cu(II)-p-hydroquinonate polymer. *Crystengcomm*, Vol.13, No.2, pp. 391-395, ISSN 1466-8033

Philibert, A., Thomas, F., Philouze, C., Hamman, S., Saint-Aman, E. & Pierre, J.L., (2003). Galactose oxidase models: Tuning the properties of Cu-II-phenoxyl radicals. *Chemistry-a European Journal*, Vol.9, No.16, (Aug), pp. 3803-3812, ISSN 0947-6539

Pierpont, C.G., (2001). Redox isomerism for quinone complexes of chromium and chromium oxidation state assignment from X-ray absorption spectroscopy. *Inorganic Chemistry*, Vol.40, No.22, (Oct), pp. 5727-+, ISSN 0020-1669

Rath, S.P., Rajak, K.K. & Chakravorty, A., (1999). Synthesis, structure, and catecholase reaction of a vanadate ester system incorporating monoionized catechol chelation. *Inorganic Chemistry*, Vol.38, No.20, pp. 4376-4377, ISSN 0020-1669

Rheingold, A.L. & Miller, J., (2003). *Cambridge Structural Database*, pp. ISSN

Rosi, N.L., Kim, J., Eddaoudi, M., Chen, B.L., O'Keeffe, M. & Yaghi, O.M., (2005). Rod packings and metal-organic frameworks constructed from rod-shaped secondary building units. *Journal of the American Chemical Society*, Vol.127, No.5, (Feb), pp. 1504-1518, ISSN 0002-7863

Sanmartin, J., Garcia-Deibe, A.M., Fondo, M., Navarro, D. & Bermejo, M.R., (2004). Synthesis and crystal structure of a mononuclear iron(III) (eta(2)-acetato) complex of a beta-cis folded salen type ligand. *Polyhedron*, Vol.23, No.6, (Mar), pp. 963-967, ISSN 0277-5387

Sembiring, S.B., Colbran, S.B. & Craig, D.C., (1999). Synthesis and electrochemistry of platinum complexes of hydroquinon-2-ylmethyl- and p-benzoquinon-2-ylmethyl-diphenylphosphine. *Journal of the Chemical Society-Dalton Transactions*, No.10, (May), pp. 1543-1554, ISSN 0300-9246

Sembiring, S.B., Colbran, S.B., Craig, D.C. & Scudder, M.L., (1995). Palladium(II) 2-diphenylphosphinohydroquinone (H(2)PPHQ) complexes - preparation and structures of a novel cluster, (PDBR(HPPHQ))(4) CENTER-DOT-2H2O, and a phosphine-phosphite complex, cis- PDBR2(C6H3(OH)-1,PPH(2)-3,PPH(2)O-4) CENTER-DOT-2H(2)O. *Journal of the Chemical Society-Dalton Transactions*, No.22, (Nov), pp. 3731-3741, ISSN 0300-9246

Sembiring, S.B., Colbran, S.B. & Hanton, L.R., (1992). The preparation, properties and x-ray crystal-structure of the nickel(II) hydroquinonylphosphine complex cis NI(PPHQH)2 .H2O.2(CH3)2NCHO. *Inorganica Chimica Acta*, Vol.202, No.1, (Dec), pp. 67-72, ISSN 0020-1693

Senge, M.O., Speck, M., Wiehe, A., Dieks, H., Aguirre, S. & Kurreck, H., (1999). Structure and conformation of photosynthetic pigments and related compounds. 12. A crystallographic analysis of porphyrin-quinones and their precursors. *Photochemistry and Photobiology*, Vol.70, No.2, (Aug), pp. 206-216, ISSN 0031-8655

Song, Y.F., van Albada, G.A., Tang, J., Mutikainen, I., Turpeinen, U., Massera, C., Roubeau, O., Costa, J.S., Gamez, P. & Reedijk, J., (2007). Controlled copper-mediated chlorination of phenol rings under mild conditions. *Inorganic Chemistry*, Vol.46, No.12, (Jun), pp. 4944-4950, ISSN 0020-1669

Sreenivasulu, B., Zhao, F., Gao, S. & Vittal, J.J., (2006). Synthesis, structures and catecholase activity of a new series of dicopper(II) complexes of reduced Schiff base ligands. *European Journal of Inorganic Chemistry*, No.13, (Jul), pp. 2656-2670, ISSN 1434-1948

Stobie, K.M., Bell, Z.R., Munhoven, T.W., Maher, J.P., McCleverty, J.A., Ward, M.D., McInnes, E.J.L., Totti, F. & Gatteschi, D., (2003). Mono- and di-nuclear tris(pyrazolyl)borato-oxo-tungsten(v) complexes with phenolate ligands: syntheses and structures, and magnetic, electrochemical and UV/Vis/NIR spectroscopic properties. *Dalton Transactions*, No.1, pp. 36-45, ISSN 1477-9226

Stylianou, M., Drouza, C., Athanasopoulos, G.I., Giapintzakis, J. & Keramidas, A.D., (2011). Vanadium(IV)-hydroquinonate radical traps towards the investigation of dioxygen activation from vanadium complexes at acidic pHs. *Submitted*, pp. ISSN

Stylianou, M., Drouza, C., Viskadourakis, Z., Giapintzakis, J. & Keramidas, A.D., (2008). Synthesis, structure, magnetic properties and aqueous solution characterization of p-hydroquinone and phenol iminodiacetate copper(II) complexes. *Dalton Transactions*, No.44, pp. 6188-6204, ISSN 1477-9226

Stylianou, M., Keramidas, A.D. & Drouza, C., (2010). PH-potentiometric investigation towards chelating tendencies of p -hydroquinone and phenol iminodiacetate copper(II) complexes. *Bioinorganic Chemistry and Applications*, Vol.2010, pp. ISSN 1565-3633

Tanski, J.M., Vaid, T.P., Lobkovsky, E.B. & Wolczanski, P.T., (2000). Covalent metal-organic networks: Pyridines induce 2-dimensional oligomerization of (mu-OC6H4O)(2)Mpy(2) (M = Ti, V, Zr). *Inorganic Chemistry*, Vol.39, No.21, (Oct), pp. 4756-4765, ISSN 0020-1669

Tanski, J.M. & Wolczanski, P.T., (2001). A covalent vanadium(III) 2-dimensional network and vanadyl chains linked by aryldioxides. *Inorganic Chemistry*, Vol.40, No.2, (Jan), pp. 346-353, ISSN 0020-1669

Ung, V.A., Bardwell, D.A., Jeffery, J.C., Maher, J.P., McCleverty, J.A., Ward, M.D. & Williamson, A., (1996). Dinuclear oxomolybdenum(V) complexes showing strong interactions across diphenol bridging ligands: Syntheses, structures, electrochemical properties, and EPR spectroscopic properties. *Inorganic Chemistry*, Vol.35, No.18, (Aug), pp. 5290-5299, ISSN 0020-1669

Ung, V.A., Couchman, S.M., Jeffery, J.C., McCleverty, J.A., Ward, M.D., Totti, F. & Gatteschi, D., (1999). Electrochemical and magnetic exchange interactions in trinuclear chain complexes containing Oxo-Mo(V) fragments as a function of the topology of the bridging ligand. *Inorganic Chemistry*, Vol.38, No.2, (Jan), pp. 365-369, ISSN 0020-1669

Vaid, T.P., Lobkovsky, E.B. & Wolczanski, P.T., (1997). Covalent 3- and 2-dimensional titanium-quinone networks. *Journal of the American Chemical Society*, Vol.119, No.37, (Sep), pp. 8742-8743, ISSN 0002-7863

Vaid, T.P., Sydora, O.L., Douthwaite, R.E., Wolczanski, P.T. & Lobkovsky, E.B., (2001). Hydrogen bonds between polyphenol (p-HOC6H4O)(6)W and bipyridines: (4,4 '-bipy center dot HOC6H4O)(6)W and 3-D networks {4,4 '-(nC(5)H(4))(2)(CH2CH2)}(n){(HOC6H4O)(6)W} (infinity) (n=2, 3). *Chemical Communications*, No.14, pp. 1300-1301, ISSN 1359-7345

Vaid, T.P., Tanski, J.M., Pette, J.M., Lobkovsky, E.B. & Wolczanski, P.T., (1999). Covalent three-dimensional titanium(IV)-aryloxide networks. *Inorganic Chemistry*, Vol.38, No.14, (Jul), pp. 3394-3405, ISSN 0020-1669

Zhang, X.Q., Huang, F.P., Bian, H.D., Yu, Q. & Liang, H., (2009). Aqua N-(2,5-dihydroxybenzyl)iminodiacetato copper(II). *Acta Crystallographica Section E-Structure Reports Online*, Vol.65, (Nov), pp. M1393-U1393, ISSN 1600-5368

Zharkouskaya, A., Buchholz, A. & Plass, W., (2005). A new coordination polymer architecture with (10,3)-a network containing chiral hydrophilic 3-D channels. *European Journal of Inorganic Chemistry*, No.24, (Dec), pp. 4875-4879, ISSN 1434-1948

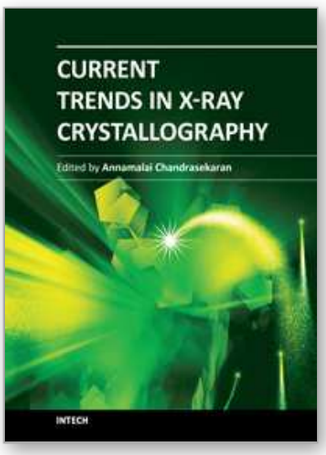

Current Trends in X-Ray Crystallography

Edited by Dr. Annamalai Chandrasekaran

ISBN 978-953-307-754-3
Hard cover, 436 pages
Publisher InTech
Published online 16, December, 2011
Published in print edition December, 2011

This book on X-ray Crystallography is a compilation of current trends in the use of X-ray crystallography and related structural determination methods in various fields. The methods covered here include single crystal small-molecule X-ray crystallography, macromolecular (protein) single crystal X-ray crystallography, and scattering and spectroscopic complimentary methods. The fields range from simple organic compounds, metal complexes to proteins, and also cover the meta-analyses of the database for weak interactions.

How to reference

In order to correctly reference this scholarly work, feel free to copy and paste the following:

Anastasios D. Keramidas, Chryssoula Drouza and Marios Stylianou (2011). σ-Bonded p-Dioxolene Transition Metal Complexes, Current Trends in X-Ray Crystallography, Dr. Annamalai Chandrasekaran (Ed.), ISBN: 978-953-307-754-3, InTech, Available from: http://www.intechopen.com/books/current-trends-in-x-ray-crystallography/-963-bonded-p-dioxolene-transition-metal-complexes

INTECH
open science | open minds

InTech Europe
University Campus STeP Ri
Slavka Krautzeka 83/A
51000 Rijeka, Croatia
Phone: +385 (51) 770 447
Fax: +385 (51) 686 166
www.intechopen.com

InTech China
Unit 405, Office Block, Hotel Equatorial Shanghai
No.65, Yan An Road (West), Shanghai, 200040, China
中国上海市延安西路65号上海国际贵都大饭店办公楼405单元
Phone: +86-21-62489820
Fax: +86-21-62489821

IntechOpen